

The novel ECM protein SNED1 mediates cell adhesion via $\alpha 5\beta 1$ integrin

Dharma Pally¹, Nandini Kapoor¹, Alexandra Naba^{1,2}

¹ Department of Physiology and Biophysics, University of Illinois Chicago, Illinois, 60612, USA

² University of Illinois Cancer Center, Chicago, Illinois, 60612, USA

Correspondence: anaba@uic.edu

Running title: SNED1 mediates cell adhesion

Keywords: Cell-ECM interactions, ECM receptors, Breast cancer metastasis, Neural crest cells, RGD motif, Matrisome

ABSTRACT

The extracellular matrix (ECM) is a complex meshwork comprising over 100 proteins. It serves as an adhesive substrate for cells and, hence, plays critical roles in health and disease. We have recently identified a novel ECM protein, SNED1, and have found that it is required for neural crest cell migration and craniofacial morphogenesis during development and in breast cancer, where it is necessary for the metastatic dissemination of tumor cells. Interestingly, both processes involve the dynamic remodeling of cell-ECM adhesions via cell surface receptors. Sequence analysis revealed that SNED1 contains two amino acid motifs, RGD and LDV, known to bind integrins, the largest class of ECM receptors. We thus sought to investigate the role of SNED1 in cell adhesion. Here, we report that SNED1 mediates breast cancer and neural crest cell adhesion via its RGD motif. We further demonstrate that cell adhesion to SNED1 is mediated by $\alpha 5\beta 1$ integrin. These findings are a first step toward identifying the signaling pathways activated downstream of the SNED1-integrin interactions guiding craniofacial morphogenesis and breast cancer metastasis.

SUMMARY STATEMENT

We report that the novel ECM protein SNED1 promotes the adhesion of breast cancer and neural crest cells via interaction with $\alpha 5\beta 1$ integrin, the first SNED1 receptor identified to date.

INTRODUCTION

The extracellular matrix (ECM), a fundamental component of multicellular organisms, is a complex 3-dimensional (3D) meshwork consisting of over a hundred proteins (Hynes and Naba, 2012; Naba, 2024). The primary function of the ECM is to serve as a substrate for cell adhesion (Hynes, 2009). The adhesion of cells to their surrounding ECM is mediated by cell-surface receptors and is critical for cell survival, as detachment from the ECM results in apoptotic cell death, known as anoikis (Frisch and Francis, 1994). In addition, cell-ECM interactions trigger molecular events that regulate a multitude of cellular phenotypes including migration (Dzamba and DeSimone, 2018; Pally and Naba, 2024), proliferation (Hynes, 2009), and differentiation (Walma and Yamada, 2020). As a result, alterations of cell-ECM adhesions and downstream signaling pathways lead to developmental defects (Rozario and DeSimone, 2010) and pathologies like cancer (Cox, 2021; Pickup et al., 2014) and fibrosis (Herrera et al., 2018). Yet, only a small subset of the hundreds of proteins comprising the matrisome is the focus of active investigations, and the mechanisms by which they interact with cells and guide cell phenotype are known for an even smaller subset.

One such understudied ECM protein is Sushi, Nidogen, and EGF like Domains 1 (SNED1). The murine gene *Sned1* was cloned two decades ago (Leimeister et al., 2004), however, it took ten years to identify its first function as a promoter of breast cancer metastasis (Naba et al., 2014). Beyond its role in breast cancer, we recently reported that *Sned1* is an essential gene, as knocking it out resulted in early neonatal lethality and severe craniofacial malformations (Barqué et al., 2021). We further showed that knocking out *Sned1* specifically from neural crest cells, the cell population that contributes to forming most craniofacial features (Mankarious and Goudy, 2010; Martik and Bronner, 2021; Trainor, 2005), was sufficient to recapitulate the craniofacial phenotype observed upon global *Sned1* deletion, demonstrating a new role for SNED1 in craniofacial morphogenesis (Barqué et al., 2021). However, as of today, the mechanisms through which SNED1 interacts with cells to mediate its phenotypes remain unknown. Of note, metastatic breast cancer cells and neural crest cells share common features (Gallik et al., 2017), including their ability to remodel their adhesions to acquire increased migratory potential (Doyle et al., 2022; Gallik et al., 2017; Mayor and Theveneau, 2013; Tucker et al., 1988). This process is, in part,

mediated by integrins, which are the main class of ECM receptors (Bökel and Brown, 2002; Campbell and Humphries, 2011; Hood and Cheresh, 2002; Hynes, 2002; Kanchanawong and Calderwood, 2023). For example, *in vivo* and *in vitro* experiments have demonstrated that $\beta 1$ integrins at the surface of neural crest cells interact with the ECM and ECM proteins like fibronectin to promote cell adhesion and subsequent migration (Alfandari et al., 2003; Duband et al., 1991; Leonard and Taneyhill, 2020; Pietri et al., 2004; Testaz et al., 1999; Yang et al., 1993). $\beta 1$ -containing integrin heterodimers expressed by breast cancer cells have been shown to interact with the vascular ECM to promote extravasation during metastasis (Chen et al., 2016) and be essential to every step of the metastatic cascade (Hamidi and Ivaska, 2018). Interestingly, SNED1 contains two putative integrin-binding motifs, an arginine-glycine-aspartic acid (RGD) triplet and a leucine-aspartic acid-valine (LDV) triplet, known in other proteins to mediate cell-ECM adhesion. We thus sought to determine whether SNED1 played a role in cell adhesion.

Here we report that SNED1 mediates the adhesion of breast cancer cells and neural crest cells, two cell types of relevance to the *in-vivo* functions of SNED1. Using a combination of genetic and pharmacological approaches, we further show that cell adhesion to SNED1 is mediated by its RGD motif and the engagement of $\alpha 5\beta 1$ integrins. Our study is thus the first to report the identification of a SNED1 receptor and constitutes an important step toward the identification of the biochemical signaling events leading to SNED1-dependent breast cancer metastasis and craniofacial development.

RESULTS AND DISCUSSION

SNED1 mediates breast cancer and neural crest cell adhesion

We first sought to determine whether SNED1 could mediate cell adhesion. To do so, we seeded highly metastatic MDA-MB-231 ‘LM2’ breast cancer cells (further termed LM2) or O9-1 neural crest cells on surfaces coated with increasing concentrations of purified human SNED1 (Vallet et al., 2021) (Fig S1A) or murine *Sned1*, respectively, and allowed cells to adhere for 30 min. Cell adhesion was assayed using a crystal-violet-based colorimetric assay and we found that SNED1 mediated the adhesion of LM2 breast cancer cells and O9-1 neural crest cells in a concentration-dependent manner with maximum adhesion observed at 10 $\mu\text{g}/\text{mL}$ concentration (Fig 1A and B, respectively). At this concentration, SNED1 exerted the same adhesive properties as fibronectin toward these two cell populations (represented by 100% adhesion). We further showed that the O9-1 cells, which are of murine origin, adhered in the same proportion to both murine *Sned1* and human SNED1 (Fig S1B). *Sned1* also mediated the adhesion of immortalized mouse embryonic fibroblasts derived from *Sned1* knockout mice (*Sned1*^{KO} iMEFs) to the same extent as the other two cell lines (Fig S1C). Altogether these experiments demonstrate that SNED1 mediates cell adhesion and exerts adhesive properties toward a panel of cell types.

The N-terminal region of SNED1 is sufficient to mediate cell adhesion

SNED1 is a modular protein composed of different domains, including a NIDO domain, a follistatin domain, and a sushi domain (also known as complement control protein or CCP domain), in addition to multiple repeats of EGF-like (EGF), calcium-binding EGF-like (EGF-Ca), and fibronectin type 3 (FN3) domains, all involved in protein-protein interactions (Fig 2A). To assess which region(s) of SNED1 mediate cell adhesion, we generated and purified three truncated forms of SNED1 (Fig 2A): the SNED1¹⁻⁷⁵¹ form lacks the C-terminal region that comprises three FN3 domains, shown to mediate cell adhesion in other ECM proteins, and the most C-terminal EGF-like domains; the SNED1¹⁻⁵³⁰ fragment additionally lacks the sushi domain and EGF-like domains after the follistatin domain; the SNED1¹⁻²⁶⁰ construct encompasses the very N-terminal region, including a single NIDO domain, which is only present in four other proteins in the human and mouse proteomes (nidogen-1 and nidogen-2, alpha-tectorin, and mucin-4) and its function

remains unknown (Barqué et al., 2021). These synthetic constructs were designed to include adequate domain boundaries to ensure proper folding and secretion (Fig 2B).

Using these purified truncated proteins as substrates, we found that LM2 cells had a decreased ability to adhere to SNED1¹⁻⁷⁵¹ and SNED1¹⁻⁵³⁰ as compared to full-length SNED1 (1.4- and 1.75-fold decrease, respectively; Fig 2C). Similarly, we observed that O9-1 cells had a decreased ability to adhere to SNED1¹⁻⁷⁵¹ and SNED1¹⁻⁵³⁰ compared to full-length SNED1 (1.58- and 1.7-fold decrease, respectively; Fig 2D). Notably, although SNED1¹⁻⁵³⁰ further lacks the sushi domain and four EGF-like domains, along with the domains absent in SNED1¹⁻⁷⁵⁰, it mediated cell adhesion to the same extent as SNED1¹⁻⁷⁵⁰ for both cell lines (Fig 2C and D). Interestingly, LM2 and O9-1 cells could adhere to the shortest N-terminal SNED1¹⁻²⁶⁰ fragment in a similar proportion as to full-length SNED1 (Fig 2C and D, respectively). Altogether, these results indicate that the adhesive property of SNED1 is primarily mediated by its N-terminal region. These results also suggests that the three FN3 domains and the EGF-like domains lacking in the SNED1¹⁻⁷⁵¹ and SNED1¹⁻⁵³⁰ constructs are required for full length SNED1 to adopt a conformation where the N-terminal adhesive site is fully accessible to cells, since their absence resulted in decreased cell adhesion.

SNED1 mediates cell adhesion via its RGD motif

Analysis of the SNED1 sequence has revealed the presence of two putative integrin binding motifs: RGD and LDV. These motifs were discovered in other ECM proteins, such as fibronectin and thrombospondin 1, and interact with integrin heterodimers at the cell surface to mediate cell adhesion (Lawler et al., 1988; Ruoslahti and Pierschbacher, 1987).

To determine whether the RGD and LDV motifs of SNED1 are required for cell adhesion, we mutated these sites alone or in combination (p40D>E in the RGD motif; p311D>A in the LDV motif; Fig 3A). Similar mutations in other ECM proteins have been shown to disrupt their interaction with integrin heterodimers (Cherny et al., 1993; Pytela et al., 1985). We next expressed these constructs in 293T cells and purified the corresponding secreted proteins from the conditioned culture medium using affinity chromatography (Fig S2). Purified proteins were then used to perform cell adhesion assays. We observed that LM2 cells showed a statistically significant decrease in their ability to adhere to SNED1^{RGE} and SNED1^{RGE/LAV} as compared to SNED1^{WT} (3- and 2.5-fold decrease, respectively; Fig 3B). Similarly, O9-1 cells showed a significant decrease

in their ability to adhere to SNED1^{RGE} and SNED1^{RGE/LAV} as compared to SNED1^{WT} (4- and 5.5-fold decrease, respectively; Fig 3C). However, mutation of the LDV motif to LAV did not affect cell adhesion (Fig 3B, C). These results demonstrate that the RGD but not the LDV motif in SNED1 is required for cell adhesion.

Functional inhibition of integrin $\alpha 5\beta 1$ significantly reduces breast cancer and neural crest cell adhesion to SNED1

To complement this set of observations and determine whether integrins mediate adhesion to SNED1, we performed experiments aimed at targeting the ability of integrins to interact with SNED1. First, we performed adhesion assays in the presence of cyclic RGDfV (cRGDfV) peptide, a peptide known to bind with high affinity to integrins that engage with the RGD motif of ECM proteins (Aumailley et al., 1991). We observed reduced adhesion of both LM2 (Fig 4A) and O9-1 cells (Fig 4B) in a concentration-dependent manner in presence of cRGDfV as compared to vehicle-treated cells. Since we previously showed that the N-terminal region of SNED1 was sufficient to mediate cell adhesion and the RGD motif is located within this fragment, we evaluated the ability of cells to adhere to SNED1¹⁻²⁶⁰ in presence of 10 μ M of cRGDfV peptide. We found that this integrin inhibitor fully abrogated LM2 and O9-1 cell adhesion (Fig S3A, B). This result suggests that the adhesive property of SNED1¹⁻²⁶⁰ is solely mediated by the RGD motif and not the NIDO domain.

The cRGDfV peptide inhibits a panel of RGD-binding integrin heterodimers such as $\alpha v\beta 3$, $\alpha v\beta 6$, $\alpha 5\beta 1$, and $\alpha v\beta 5$ (Kapp et al., 2017). Using *in silico* molecular modeling, we previously predicted that SNED1 could potentially interact with 11 integrin subunits, $\alpha 1$, $\alpha 4$, $\alpha 7$, $\alpha 10$, $\alpha 11$, $\beta 1$, $\beta 2$, $\beta 3$, $\beta 4$, $\beta 5$, and $\beta 7$ (Vallet et al., 2021) forming six functional heterodimers: $\alpha 1\beta 1$, $\alpha 4\beta 1$, $\alpha 7\beta 1$, $\alpha 10\beta 1$, $\alpha 11\beta 1$, and $\alpha 4\beta 7$ (Hynes, 2002) including the RGD-binding integrin $\alpha 5\beta 1$ (Fig 4C). We thus tested whether cell adhesion to SNED1 was dependent on $\alpha 5\beta 1$ integrin. We first confirmed that LM2 and O9-1 cells expressed $\alpha 5\beta 1$ integrin (Fig 4D). We then performed cell adhesion assays in presence of functional blocking antibodies targeting $\beta 1$ and $\alpha 5$ integrins and demonstrated that the adhesion of LM2 cells (Fig 4E) and O9-1 cells (Fig 4F) to SNED1 was significantly reduced in presence of antibodies targeting $\beta 1$ integrin (52% and 41% decrease,

respectively, as compared to isotype controls) or $\alpha 5$ integrin (30% and 9% decrease, respectively, as compared to isotype controls). This result is in line with our observation of decreased cell adhesion to SNED1^{RGE}. Altogether, these experiments identified $\alpha 5\beta 1$ integrin as the first SNED1 receptor.

It is worth noting that inhibition of $\alpha 5$ or $\beta 1$ integrins did not fully abrogate cell adhesion to SNED1, suggesting that there are likely additional integrin and non-integrin SNED1 receptors at the surface of these cells. Indeed, we have previously shown using *in-silico* prediction, that SNED1 could interact with 55 transmembrane proteins, in addition to integrins, including the basal cell adhesion molecule (BCAM) or dystroglycan 1 (DAG1), two known ECM receptors (Vallet et al., 2021). The identification of these receptors at the surface of breast cancer cells and neural crest cells will be the focus of future studies.

While our results demonstrate that the RGD motif mediates breast cancer and neural crest cell adhesion, they also raise questions on the role of the LDV motif in SNED1. The LDV motif is primarily recognized by $\alpha 4\beta 1$ and $\alpha 4\beta 7$ integrins that are mainly expressed by leukocytes. Integrin $\alpha 4$ has been previously demonstrated to play a vital role in neural crest cell migration (Kil et al., 1998) and cancer cell adhesion to the vascular endothelium (Taichman et al., 1991). Here, we show that $\alpha 4$ is expressed by LM2 and O9-1 cells (Fig S4A); however, functional blocking of integrin $\alpha 4$ did not affect the adhesion of LM2 cells to SNED1 (Fig S4B), in line with our observation that these cells could adhere similarly to SNED1^{LAV} and SNED1^{WT}. This is also in line with the observation that the two truncated forms of SNED1, SNED1¹⁻⁵³⁰ and SNED1¹⁻⁷⁵¹, which contain the LDV motif, are not sufficient to mediate cell adhesion. This opens the possibility that SNED1, via its LDV motif, could engage other cell populations in other pathophysiological processes that have yet to be discovered.

In addition to mediating cell adhesion, integrin heterodimers are involved in the early steps of ECM assembly; for example, $\alpha 5\beta 1$ integrin is critical for the initiation of fibronectin fibrillogenesis (Mao and Schwarzbauer, 2005). We have previously shown that SNED1 forms fibers in the ECM (Vallet et al., 2021), yet we do not know the mechanisms required for this process. It will thus be interesting to determine if $\alpha 5\beta 1$ integrin also mediates SNED1 fiber assembly.

Finally, given the critical role integrin-ECM interactions play in driving pathological processes, devising therapeutic strategies to prevent or disrupt these interactions is an active area of investigation (Hamidi et al., 2016; Pang et al., 2023; Raab-Westphal et al., 2017). To date, seven small molecule inhibitors and biologics have been successfully marketed, including monoclonal antibodies specifically blocking $\alpha4\beta7$ and $\alpha4\beta1$ to treat inflammatory disorders such as ulcerative colitis, Crohn's disease, and multiple sclerosis (Pang et al., 2023; Slack et al., 2022). Our study has thus the potential to pave the way to devise novel therapeutic strategies aimed at targeting SNED1- $\alpha5\beta1$ integrin interaction to prevent breast cancer metastasis.

MATERIALS AND METHODS

Plasmid constructs

The cDNA encoding full-length human SNED1 cloned into pCMV-XL5 was obtained from Origene (clone SC315884). 6X-His-tagged SNED1 previously described (Vallet et al., 2021) was subcloned into the bicistronic retroviral vector pMSCV-IRES-Hygromycin between the BglIII and HpaI sites. FLAG-tagged SNED1 was previously described (Vallet et al., 2021).

Site-directed mutagenesis to generate SNED1^{RGE} (c.C120A; p.D40E) and SNED1^{LAV} (c.A932C; p.D311A) was performed using the QuikChange kit (Agilent #200519) following the manufacturer's instructions using the cDNA encoding SNED1 from Origene as a template. To obtain the double mutant SNED1^{RGE/LAV} (c.C120A; p.D40E / c.A932C; p.D311A), we introduced the c.C120A mutation in the c.A932C mutant. These constructs were then subcloned into the bicistronic retroviral vector pMSCV-IRES-Hygromycin between the BglIII and HpaI sites, and a 6X-Hix-tag was introduced by PCR in 3' (C-terminus of the protein).

Truncated forms of human SNED1 were subcloned by PCR to generate the following fragments: SNED1¹⁻⁵³⁰, encompassing the N-terminal region of SNED1 until the follistatin domain, and SNED1¹⁻⁷⁵¹, encompassing the N-terminal region of SNED1 until the sushi domain (Fig 2A). These constructs were then subcloned into the bicistronic retroviral vector pMSCV-IRES-Hygromycin between the BglIII and HpaI sites, and a FLAG tag (DYKDDDDK) was added at the C-terminus via PCR as previously described (Vallet et al., 2021). FLAG-tagged SNED1¹⁻²⁶⁰, encompassing the very N-terminal region of SNED1 was previously described (Vallet et al., 2021). The sequences of the primers used to introduce point mutations or generate truncated fragments of SNED1 are listed in Supplementary Table 1. All constructs were verified by sequencing.

Cell culture

Cell maintenance

Highly metastatic breast cancer cells, MDA-MB-231 'LM2' (termed LM2 in the manuscript), were kindly gifted by Dr. Joan Massagué (Memorial Sloan Kettering Cancer Center, New York, NY). LM2 cells, human embryonic kidney 293T cells (termed 293T in the manuscript) stably overexpressing different constructs of SNED1, and immortalized mouse embryonic fibroblasts isolated from *Sned1*^{KO} mice (*Sned1*^{KO} iMEFs) (Vallet et al., 2021) were cultured in Dulbecco's

Modified Eagle's medium (DMEM; Corning, #10-017-CV) supplemented with 10% fetal bovine serum (FBS; Sigma, #F0926) and 2 mM glutamine (Corning, #25-005-CI); this formulation is termed "complete medium" in this manuscript. The O9-1 mouse cranial neural crest cell line (Millipore Sigma, #SCC049) was cultured per the manufacturer's instructions. Briefly, cells were cultured on dishes coated with Matrigel® (Corning, #356234) prepared at 0.18 mg/mL in 1X Dulbecco's Phosphate Buffered Saline (D-PBS) containing calcium and magnesium (Cytiva, #SH30264.FS) in presence of complete ES cell medium containing 15% FBS and leukemia inhibitory factor (Millipore Sigma, #ES-101-B) and supplemented with 25 ng/mL fibroblast growth factor-2 (FGF-2, R&D systems, #233-FB). All cell lines were maintained at 37°C in a 5% CO₂ humidified incubator.

Retrovirus production

293T cells were plated at ~ 30% confluency in a 6-well plate. Cells were transfected the following day using a Lipofectamine 3000 (Invitrogen, #L3000-008) mixture containing 1 µg of a retroviral vector with the construct of interest and 0.5 µg each of a packaging vector (pCL-Gag/Pol) and a vector encoding the VSVG coat protein prepared in Opti-MEM™ (Gibco, #31985070). After 24h, the transfection mixture was replaced with fresh complete medium, and cells were cultured for an additional 24h, after which the conditioned medium containing viral particles was collected, passed through 0.45 µ filter, and then either immediately used for cell transduction or stored at -80°C for later use.

Generation of 293T cells stably expressing SNED1 constructs.

293T cells were seeded at ~30% confluency. The following day, cells were transduced with undiluted viral particles-containing conditioned medium. 24h after transduction, the medium was replaced with fresh complete medium, and cells were allowed to grow for another 24h before selection with hygromycin (100 µg/mL). Once stable cell lines were established, we assessed the production and secretion of recombinant proteins using immunoblotting of total cell extract (TCE) and conditioned medium, respectively, using either an anti-SNED1, anti-His or anti-FLAG antibody.

Protein purification

Condition medium collection

293T cells stably expressing constructs of interest were seeded in a 15 cm dish in complete medium and allowed to grow until reaching 100% confluency. The culture medium was aspirated, the monolayer was rinsed with 1X D-PBS containing calcium and magnesium, and the medium was replaced with serum-free DMEM medium supplemented with 2 mM glutamine for 48h. The serum-free conditioned medium (CM) containing secreted SNED1 was harvested, and cells were allowed to recover for 48h in complete medium before repeating the next cycle. Cells were discarded after five cycles. An EDTA-free protease inhibitor cocktail (0.067X final concentration; Thermo Scientific, #A32955) was added to the CM, and the CM was centrifuged at 4000 rpm for 10 min to remove any cell or cellular debris. Pre-cleared supernatants were collected and stored at -80°C until further processing.

Metal affinity purification of His-tagged SNED1 proteins

6X His-tagged SNED1 proteins (wild-type or integrin-binding mutants) were purified via immobilized metal affinity chromatography (IMAC) using an AKTA Pure system for fast protein liquid chromatography (FPLC) at the UIC Biophysics Core Facility. In brief, conditioned medium (CM) containing the secreted protein of interest was thawed at 4°C, concentrated using a 100-kDa protein concentrator with a polyethersulfone membrane (Thermo Scientific, #88537), buffer-exchanged against a binding buffer containing 20 mM Tris, 500 mM NaCl, 20 mM imidazole (pH 7.5), and filtered using a 0.2 µm filter. In parallel, a HisTrap HP column (column volume: 1 mL) was equilibrated with the binding buffer. The filtered CM was applied to the equilibrated HisTrap column to allow protein binding. The column was then washed with 20 column volumes of binding buffer and bound proteins were eluted with a buffer containing 20 mM Tris-HCl, 500 mM NaCl, 5 mM β-mercaptoethanol (pH 7.5), and a stepwise gradient of increasing imidazole concentration (12.5mM, 50mM, 125mM, 250mM, 375mM, and 500mM). The elution fractions were concentrated, and a buffer exchange was performed with HEPES Buffered Saline (HBS; 10 mM HEPES, 150 mM NaCl, pH 7.5).

Purification of FLAG-tagged SNED1 proteins

Since we could not achieve sufficient purity of His-tagged truncated forms of SNED1, we cloned FLAG-tagged versions of these proteins for purification (Fig 2B) In brief, conditioned medium containing FLAG-tagged full-length or truncated forms of SNED1 was thawed at 4°C overnight and concentrated using protein concentrators with a 10kDa weight cut-off for the SNED1¹⁻²⁶⁰ and SNED1¹⁻⁵³⁰ fragments (Thermo Scientific, #88535), a 30kDa cut-off for the SNED1¹⁻⁷⁵¹ fragment (Thermo Scientific, #88536), and a 100kDa cut-off for full-length SNED1 (Thermo Scientific, #88537). An anti-FLAG resin (Sigma, #A220), containing monoclonal M2 anti-FLAG antibodies coupled to agarose beads was washed with 20 column volumes of HBS twice. Concentrated CM was applied to the resin and incubated overnight under constant rotation at 4°C to allow protein binding. The following day, the unbound fraction was collected, and the resin was washed with 20 column volumes of HBS thrice. Bound FLAG-tagged proteins were eluted by competing with 200 µg/mL of FLAG peptide in HBS in a stepwise manner, resulting in 4 elution fractions. Protein fractions were then pooled, and buffer-exchanged with HBS using protein concentrators of appropriate molecular weight cut-off (see above) to remove the excess of unbound FLAG peptide.

Protein quantification and quality assessment

Purified proteins were quantified by measuring the absorbance at $\lambda=280$ nm using a NanoDrop spectrophotometer. To assess their quality and purity, proteins were resolved by electrophoresis on polyacrylamide gels. Gels were stained overnight using Coomassie-based AquaStain (Bulldog, #AS001000) and imaged with a ChemiDoc MP™ imaging system (Bio-Rad).

Adhesion assay

Substrate coating

Adhesion assays were performed as described previously (Humphries, 1998). In brief, wells of a 96-well plate were coated with 50 µL of different concentrations, ranging from 0.1 µg/mL to 10 µg/mL, of purified human SNED1 proteins (full-length, fragments, or integrin-binding mutants) or murine Sned1 (R&D systems, 9335-SN) for 180 min at 37°C. Fibronectin (5 µg/mL; Millipore, #FC010) was used as a positive control. The adsorbed protein was immobilized with 0.5% (v/v) glutaraldehyde for 15 min at room temperature (RT). To prevent cell adhesion to plastic, wells

were blocked using 200 μ L of 10 mg/mL heat-denatured bovine albumin serum (BSA; Sigma, #A9576). Uncoated wells blocked with BSA (10 mg/mL) alone were used as a negative control.

Cell seeding and crystal violet assay

Single-cell suspension of LM2 or O9-1 cells containing 5×10^5 cells/mL were prepared in complete medium. 25,000 cells were added to each well and allowed to adhere for 30 min at 37°C. Loosely attached or non-adherent cells were removed by gently washing the wells with 100 μ L of D-PBS⁺⁺ thrice and fixed using 100 μ L of 5% (v/v) glutaraldehyde for 30 minutes at RT. Cells were stained with 100 μ L of 0.1% (w/v) crystal violet in 200 mM 2-(N-morpholino)ethanesulfonic acid (MES), pH 6.0 for 60 min at RT. After washing the excess of unbound crystal violet, the dye was solubilized in 10% (v/v) acetic acid. Absorbance values were measured at $\lambda = 570$ nm using a Bio-Tek Synergy HT microplate reader. Cell adhesion was determined by interpolating the absorbance values from a standard curve that was generated by seeding cells at several dilutions (10%-100%) from the single cell suspension on poly-L-lysine (0.01% w/v; Sigma, P4707) coated wells and fixed directly by adding 5% (v/v) glutaraldehyde.

Integrin-blocking experiments were performed by seeding cells on a SNED1 substrate (10 μ g/mL) in presence of a cyclic RGDfV peptide (cRGDfV; Sigma, #SCP0111) at concentrations ranging between 1.25 μ M and 10 μ M or in presence of 10 μ g/mL of anti- β 1, anti- α 5, or anti- α 4 integrin-blocking antibodies (see Table S2 for details).

Immunoblotting

LM2 and O9-1 cells were cultured for three days in complete medium and lysed in 3x Laemmli buffer (0.1875 M Tris-HCl, 6% SDS, 30% glycerol) containing 100 mM dithiothreitol. Cell lysates were passed through a 26^{1/2}-gauge needle to ensure complete cell lysis, and samples were boiled at 95°C for 10 min. Lysates were resolved by gel electrophoresis on polyacrylamide gels at constant current (20 mA for stacking, 25 mA for resolving). Proteins were transferred onto nitrocellulose membranes at constant voltage (100 V) for 180 min at 4°C. Membranes were incubated in 5% (w/v) non-fat milk prepared in 1X PBS + 0.1% Tween-20 (PBST) for 60 min at room temperature to prevent non-specific antibody binding and then incubated in the presence of primary anti- β 1 integrin, anti- α 5 integrin or anti- α 4 integrin antibodies (see Table S2 for details) in 5% (w/v) non-fat milk in PBST overnight at 4°C. Membranes were washed and incubated with

horseradish peroxidase (HRP)-conjugated secondary antibodies for 60 min at RT. Immunoreactive bands were detected using chemiluminescence (Thermo Scientific, #E32109) and imaged with a ChemiDoc MP™ imaging system (Bio-Rad).

Data analysis and statistics

All experiments were performed with at least three technical replicates (n) and, unless noted otherwise, repeated independently three times (N; biological replicates). Data is represented as a mean±standard deviation from three biological replicates. Unpaired Student's two-tailed *t*-test with Welch's correction or Welch and Brown-Forsythe one-way ANOVA with Dunnett's T3 correction for multiple comparisons was performed to measure statistical significance. Plots were generated using PRISM (GraphPad).

ACKNOWLEDGEMENTS

We would like to thank Dr. Hyun Lee, director of the Biophysics Core facility at UIC, and her team for their help with protein purification. We would also like to thank all the members of the Naba lab for insightful discussions.

COMPETING INTERESTS

The Naba laboratory holds a sponsored research agreement with Boehringer-Ingelheim for work not related to the content of this manuscript. AN holds consulting agreements with AbbVie, XM Therapeutics, and RA Capital.

FUNDING

This work was partly supported by the National Institute of General Medical Sciences of the National Institutes of Health [R01CA232517], an award from the UIC Chancellor's Translational Research Initiative, and a start-up fund from the Department of Physiology and Biophysics of the University of Illinois Chicago to AN. NK was supported by an award from the UIC Liberal Arts and Sciences Undergraduate Research Initiative (LASURI) and a UIC Honors College Undergraduate Research Grant.

DATA AVAILABILITY

All relevant data can be found within the article and its supplementary information. Research materials are available upon request to Dr. Naba.

REFERENCES

- Alfandari, D., Cousin, H., Gaultier, A., Hoffstrom, B. G. and DeSimone, D. W.** (2003). Integrin $\alpha\beta 1$ supports the migration of *Xenopus* cranial neural crest on fibronectin. *Developmental Biology* **260**, 449–464.
- Aumailley, M., Gurrath, M., Müller, G., Calvete, J., Timpl, R. and Kessler, H.** (1991). Arg-Gly-Asp constrained within cyclic pentapeptides Strong and selective inhibitors of cell adhesion to vitronectin and laminin fragment P1. *FEBS Letters* **291**, 50–54.
- Barqué, A., Jan, K., De La Fuente, E., Nicholas, C. L., Hynes, R. O. and Naba, A.** (2021). Knockout of the gene encoding the extracellular matrix protein SNED1 results in early neonatal lethality and craniofacial malformations. *Developmental Dynamics* **250**, 274–294.
- Bökel, C. and Brown, N. H.** (2002). Integrins in Development: Moving on, Responding to, and Sticking to the Extracellular Matrix. *Developmental Cell* **3**, 311–321.
- Campbell, I. D. and Humphries, M. J.** (2011). Integrin Structure, Activation, and Interactions. *Cold Spring Harb Perspect Biol* **3**, a004994.
- Chen, M. B., Lamar, J. M., Li, R., Hynes, R. O. and Kamm, R. D.** (2016). Elucidation of the Roles of Tumor Integrin $\beta 1$ in the Extravasation Stage of the Metastasis Cascade. *Cancer Research* **76**, 2513–2524.
- Cherny, R. C., Honan, M. A. and Thiagarajan, P.** (1993). Site-directed mutagenesis of the arginine-glycine-aspartic acid in vitronectin abolishes cell adhesion. *Journal of Biological Chemistry* **268**, 9725–9729.
- Cox, T. R.** (2021). The matrix in cancer. *Nat Rev Cancer* **21**, 217–238.
- Doyle, A. D., Nazari, S. S. and Yamada, K. M.** (2022). Cell-extracellular matrix dynamics. *Phys Biol* **19**,.
- Duband, J.-L., Dufour, S., Yamada, S. S., Yamada, K. M. and Thiery, J. P.** (1991). Neural crest cell locomotion induced by antibodies to $\beta 1$ integrins A tool for studying the roles of substratum molecular avidity and density in migration. *Journal of Cell Science* **98**, 517–532.
- Dzamba, B. J. and DeSimone, D. W.** (2018). Chapter Seven - Extracellular Matrix (ECM) and the Sculpting of Embryonic Tissues. In *Current Topics in Developmental Biology* (ed. Litscher, E. S.) and Wassarman, P. M.), pp. 245–274. Academic Press.

- Frisch, S. M. and Francis, H.** (1994). Disruption of epithelial cell-matrix interactions induces apoptosis. *J Cell Biol* **124**, 619–626.
- Gallik, K. L., Treffy, R. W., Nacke, L. M., Ahsan, K., Rocha, M., Green-Saxena, A. and Saxena, A.** (2017). Neural crest and cancer: Divergent travelers on similar paths. *Mechanisms of Development* **148**, 89–99.
- Hamidi, H. and Ivaska, J.** (2018). Every step of the way: integrins in cancer progression and metastasis. *Nat Rev Cancer* **18**, 533–548.
- Hamidi, H., Pietilä, M. and Ivaska, J.** (2016). The complexity of integrins in cancer and new scopes for therapeutic targeting. *Br. J. Cancer* **115**, 1017–1023.
- Herrera, J., Henke, C. A. and Bitterman, P. B.** (2018). Extracellular matrix as a driver of progressive fibrosis. *J Clin Invest* **128**, 45–53.
- Hood, J. D. and Cheresch, D. A.** (2002). Role of integrins in cell invasion and migration. *Nature Reviews Cancer* **2**, 91–100.
- Humphries, M. J.** (1998). Cell-Substrate Adhesion Assays. *Current Protocols in Cell Biology* **00**, 9.1.1-9.1.11.
- Hynes, R. O.** (2002). Integrins: Bidirectional, Allosteric Signaling Machines. *Cell* **110**, 673–687.
- Hynes, R. O.** (2009). The Extracellular Matrix: Not Just Pretty Fibrils. *Science* **326**, 1216–1219.
- Hynes, R. O. and Naba, A.** (2012). Overview of the Matrisome—An Inventory of Extracellular Matrix Constituents and Functions. *Cold Spring Harbor Perspectives in Biology* **4**, a004903.
- Kanchanawong, P. and Calderwood, D. A.** (2023). Organization, dynamics and mechanoregulation of integrin-mediated cell–ECM adhesions. *Nat Rev Mol Cell Biol* **24**, 142–161.
- Kapp, T. G., Rechenmacher, F., Neubauer, S., Maltsev, O. V., Cavalcanti-Adam, E. A., Zarka, R., Reuning, U., Notni, J., Wester, H.-J., Mas-Moruno, C., et al.** (2017). A Comprehensive Evaluation of the Activity and Selectivity Profile of Ligands for RGD-binding Integrins. *Sci Rep* **7**, 39805.
- Kil, S. H., Krull, C. E., Cann, G., Clegg, D. and Bronner-Fraser, M.** (1998). The $\alpha 4$ Subunit of Integrin Is Important for Neural Crest Cell Migration. *Developmental Biology* **202**, 29–42.
- Lawler, J., Weinstein, R. and Hynes, R. O.** (1988). Cell attachment to thrombospondin: the role of ARG-GLY-ASP, calcium, and integrin receptors. *J Cell Biol* **107**, 2351–2361.

- Leimeister, C., Schumacher, N., Diez, H. and Gessler, M.** (2004). Cloning and expression analysis of the mouse stroma marker Snep encoding a novel nidogen domain protein. *Developmental Dynamics* **230**, 371–377.
- Leonard, C. E. and Taneyhill, L. A.** (2020). The road best traveled: Neural crest migration upon the extracellular matrix. *Semin Cell Dev Biol* **100**, 177–185.
- Mankarious, L. A. and Goudy, S. L.** (2010). Craniofacial and upper airway development. *Paediatric Respiratory Reviews* **11**, 193–198.
- Mao, Y. and Schwarzbauer, J. E.** (2005). Fibronectin fibrillogenesis, a cell-mediated matrix assembly process. *Matrix Biology* **24**, 389–399.
- Martik, M. L. and Bronner, M. E.** (2021). Riding the crest to get a head: neural crest evolution in vertebrates. *Nat Rev Neurosci* **22**, 616–626.
- Mayor, R. and Theveneau, E.** (2013). The neural crest. *Development* **140**, 2247–2251.
- Naba, A.** (2024). Mechanisms of assembly and remodelling of the extracellular matrix. *Nat Rev Mol Cell Biol* **In press**,.
- Naba, A., Clauser, K. R., Lamar, J. M., Carr, S. A. and Hynes, R. O.** (2014). Extracellular matrix signatures of human mammary carcinoma identify novel metastasis promoters. *eLife* **3**, e01308.
- Pally, D. and Naba, A.** (2024). Extracellular matrix dynamics: A key regulator of cell migration across length-scales and systems. *Curr Opin Cell Biol* **86**, 102309.
- Pang, X., He, X., Qiu, Z., Zhang, H., Xie, R., Liu, Z., Gu, Y., Zhao, N., Xiang, Q. and Cui, Y.** (2023). Targeting integrin pathways: mechanisms and advances in therapy. *Signal Transduction and Targeted Therapy* **8**, 1.
- Pickup, M. W., Mouw, J. K. and Weaver, V. M.** (2014). The extracellular matrix modulates the hallmarks of cancer. *EMBO reports* **15**, 1243–1253.
- Pietri, T., Eder, O., Breau, M. A., Topilko, P., Blanche, M., Brakebusch, C., Fässler, R., Thiery, J.-P. and Dufour, S.** (2004). Conditional β 1-integrin gene deletion in neural crest cells causes severe developmental alterations of the peripheral nervous system. *Development* **131**, 3871–3883.
- Pytela, R., Pierschbacher, M. D. and Ruoslahti, E.** (1985). Identification and isolation of a 140 kd cell surface glycoprotein with properties expected of a fibronectin receptor. *Cell* **40**, 191–198.

- Raab-Westphal, S., Marshall, J. F. and Goodman, S. L.** (2017). Integrins as Therapeutic Targets: Successes and Cancers. *Cancers* **9**, 110.
- Rozario, T. and DeSimone, D. W.** (2010). The extracellular matrix in development and morphogenesis: A dynamic view. *Developmental Biology* **341**, 126–140.
- Ruoslahti, E. and Pierschbacher, M. D.** (1987). New perspectives in cell adhesion: RGD and integrins. *Science* **238**, 491–497.
- Slack, R. J., Macdonald, S. J. F., Roper, J. A., Jenkins, R. G. and Hatley, R. J. D.** (2022). Emerging therapeutic opportunities for integrin inhibitors. *Nature Reviews Drug Discovery* **21**, 60–78.
- Taichman, D. B., Cybulsky, M. I., Djaffar, I., Longenecker, B. M., Teixidó, J., Rice, G. E., Aruffo, A. and Bevilacqua, M. P.** (1991). Tumor cell surface alpha 4 beta 1 integrin mediates adhesion to vascular endothelium: demonstration of an interaction with the N-terminal domains of INCAM-110/VCAM-1. *Cell Regulation* **2**, 347–355.
- Testaz, S., Delannet, M. and Duband, J.** (1999). Adhesion and migration of avian neural crest cells on fibronectin require the cooperating activities of multiple integrins of the (beta)1 and (beta)3 families. *J Cell Sci* **112 (Pt 24)**, 4715–4728.
- Trainor, P. A.** (2005). Specification and patterning of neural crest cells during craniofacial development. *Brain Behav Evol* **66**, 266–280.
- Tucker, G. C., Duband, J. L., Dufour, S. and Thiery, J. P.** (1988). Cell-adhesion and substrate-adhesion molecules: their instructive roles in neural crest cell migration. *Development* **103 Suppl**, 81–94.
- Vallet, S. D., Davis, M. N., Barqué, A., Thahab, A. H., Ricard-Blum, S. and Naba, A.** (2021). Computational and experimental characterization of the novel ECM glycoprotein SNED1 and prediction of its interactome. *Biochemical Journal* **478**, 1413–1434.
- Walma, D. A. C. and Yamada, K. M.** (2020). The extracellular matrix in development. *Development* **147**, dev175596.
- Yang, J. T., Rayburn, H. and Hynes, R. O.** (1993). Embryonic mesodermal defects in $\alpha 5$ integrin-deficient mice. *Development* **119**, 1093–1105.

FIGURE LEGENDS

Figure 1. SNED1 promotes breast cancer and neural crest cell adhesion

(A) Adhesion of MDA-MB-231' LM2' breast cancer cells to purified human SNED1 is concentration-dependent.

(B) Adhesion of O9-1 mouse neural crest cells to purified murine Sned1 is concentration dependent. Data is represented as mean \pm SD from three biological experiments.

Figure 2. The N-terminal region of SNED1 mediates cell adhesion

(A) Schematic showing FLAG-tagged full-length SNED1 and the different truncated forms of SNED1 used in this study: SNED1¹⁻⁷⁵¹ encompasses the N-terminal region until the sushi domain; SNED1¹⁻⁵³⁰ encompasses the N-terminal region until the follistatin domain; SNED1¹⁻²⁶⁰ encompasses the N-terminal region until the NIDO domain.

(B) Coomassie-stained gel showing the purity of purified full-length and truncated forms of SNED1.

(C-D) Adhesion of MDA-MB-231' LM2' breast cancer cells (C) and O9-1 neural crest cells (D) to full-length and truncated forms of SNED1. Data is represented as mean \pm SD from at least two biological experiments. Welch and Brown-Forsythe one-way ANOVA with Dunnett's T3 correction for multiple comparisons was performed to determine statistical significance. ns: non-significant, * $p < 0.05$, *** $p < 0.001$.

Figure 3. The RGD motif in SNED1 is required to mediate cell adhesion

(A) Schematic of SNED1 showing the two putative integrin-binding motifs in SNED1 (³⁸RGD and ³¹⁰LDV) and the point mutations introduced to disrupt their integrin-binding activity (³⁸RGD>RGE, ³¹⁰LDV>LAV).

(B, C) Adhesion of MDA-MB-231' LM2' breast cancer cells (B) and O9-1 mouse neural crest cells (C) to wild type or integrin-binding mutants (RGE, LAV or RGE/LAV) of SNED1. Data is represented as mean \pm SD from three biological experiments. Welch and Brown-Forsythe one-way ANOVA with Dunnett's T3 correction for multiple comparisons was performed to determine statistical significance. ns: non-significant, * $p < 0.05$, ** $p < 0.01$.

Figure 4. Functional blocking of integrins decreases cell adhesion to SNED1

(A-B) Adhesion of MDA-MB-231' LM2' breast cancer cell (A) and O9-1 neural crest cells (B) to SNED1 is inhibited in presence of increasing concentrations of cRGDfV peptide. Data is

represented as mean \pm SD from three biological experiments. Welch and Brown-Forsythe one-way ANOVA with Dunnett's T3 correction for multiple comparisons was performed to determine statistical significance. * $p < 0.05$, ** $p < 0.01$.

(C) Schematic showing the seven integrin heterodimers previously predicted to interact with SNED1. Adapted from (Vallet et al., 2021).

(D) Immunoblots on total cell extract from MDA-MB-231' LM2' and O9-1 cells shows $\beta 1$ integrin (top) and $\alpha 5$ integrin (bottom) expression.

(E - F) Adhesion of MDA-MB-231' LM2' breast cancer (E) and O9-1 neural crest cells (F) to SNED1 is decreased in presence of anti- $\beta 1$ and anti- $\alpha 5$ integrin-blocking antibodies. Data is represented as mean \pm SD from three biological experiments. Unpaired Student's two-tailed t-test with Welch's correction was performed to determine statistical significance. * $p < 0.05$, ** $p < 0.01$.

SUPPLEMENTARY FIGURE LEGENDS

Figure S1. Cell adhesion on human SNED1 and murine Sned1

(A) Coomassie-blue-stained polyacrylamide gel showing the quality and purity of affinity-purified full-length SNED1-His.

(B) Murine O9-1 neural crest cells adhere to the same extent to human SNED1 and murine Sned1. Data is represented as mean \pm SD from three biological experiments. Unpaired Student's two-tailed t-test with Welch's correction was performed to test statistical significance. ns: non-significant.

(C) Graph showing the adhesion of immortalized embryonic fibroblast cells isolated from *Sned1* knockout mice (*Sned1*^{KO} iMEF) on increasing concentrations of Sned1.

Figure S2. Purification of integrin-binding mutants of SNED1

Coomassie-blue-stained polyacrylamide gels showing the quality and purity of affinity-purified His-tagged SNED1^{RGE} (A), SNED1^{LAV} (B), and SNED1^{RGE/LAV} (C). The different bands correspond to different levels of glycosylation of the proteins, as previously shown (Vallet et al., 2021)

Figure S3. The RGD motif in SNED1¹⁻²⁶⁰ is sufficient to mediate cell adhesion

Adhesion of MDA-MB-231' LM2' breast cancer cells (A) and O9-1 neural crest cells (B) to the N-terminal fragment of SNED1 (SNED1¹⁻²⁶⁰) is significantly decreased in presence of the integrin-binding cRGDfV peptide. Data is represented as mean \pm SD from three biological experiments. Unpaired Student's two-tailed t-test with Welch's correction was performed to determine statistical significance. *p<0.05, ** p<0.01.

Figure S4. Functional blocking of integrin α 4 does not affect breast cancer cell adhesion on SNED1

(A) Immunoblot on total cell extract from MDA-MB-231' LM2' and O9-1 cells showing α 4 integrin expression.

(B) Adhesion of MDA-MB-231' LM2' breast cancer cells to SNED1 is not altered in presence of anti- α 4 integrin-blocking antibody. Data is represented as mean \pm SD from three biological

experiments. Unpaired Student's two-tailed t-test with Welch's correction was performed to test statistical significance. ns: non-significant.

Figure 1. SNED1 promotes breast cancer and neural crest cell adhesion

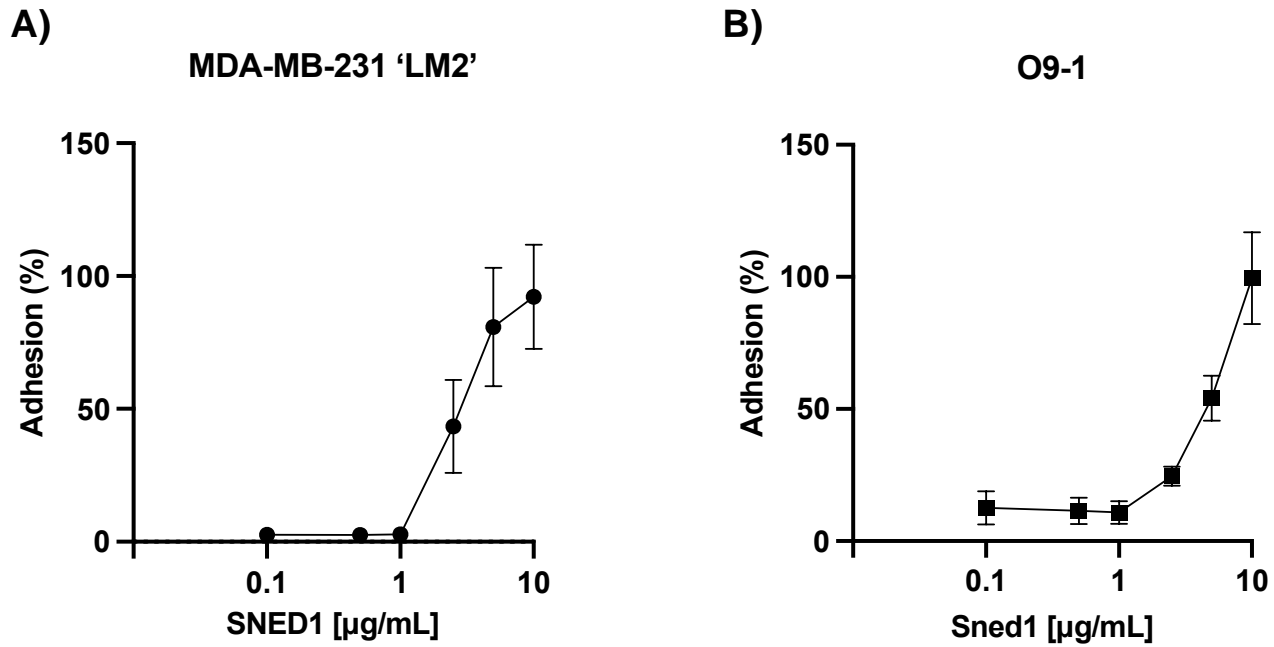


Figure 2. The N-terminal region of SNED1 mediates cell adhesion

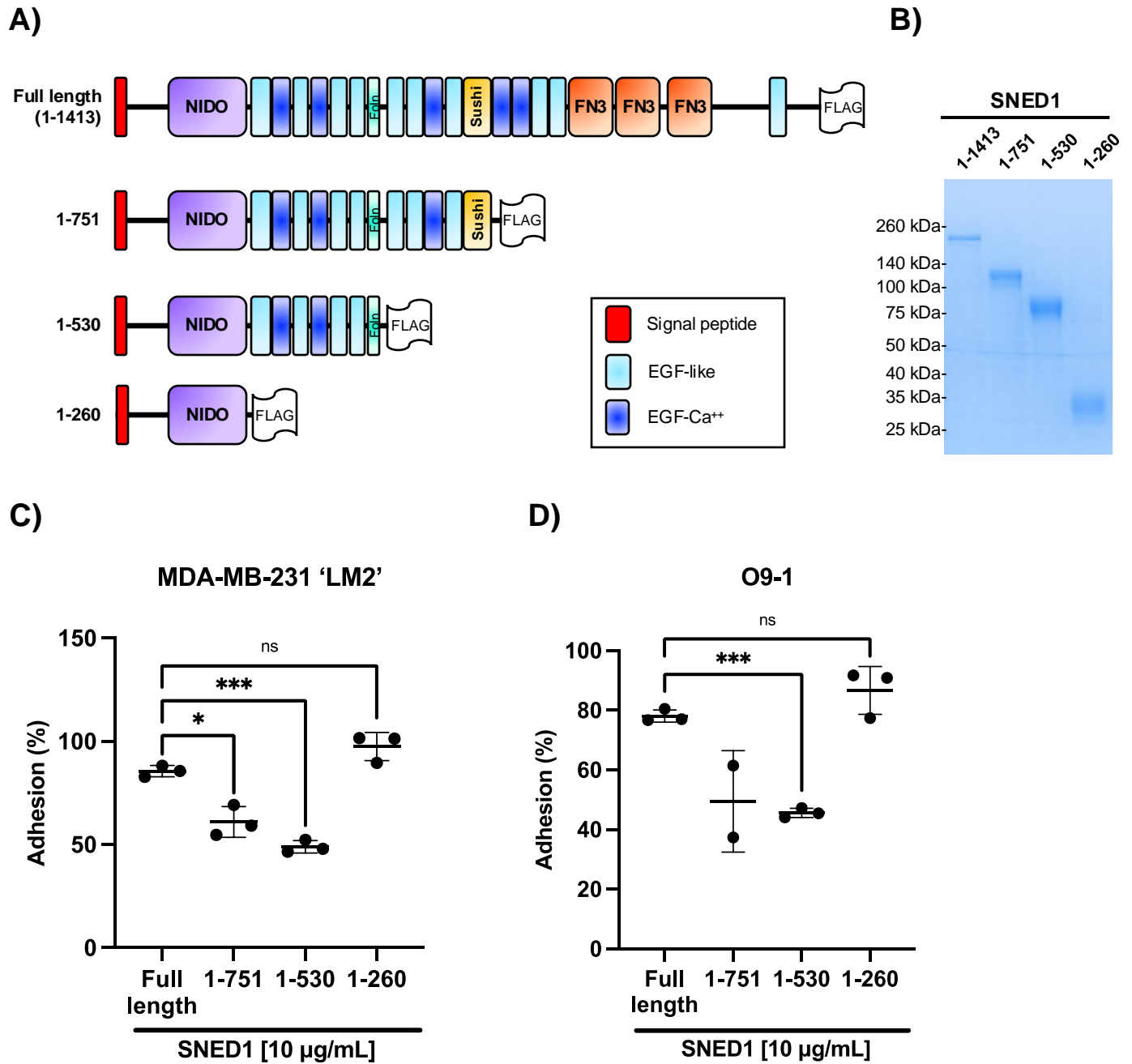


Figure 3. The RGD motif in SNED1 is required for cell adhesion

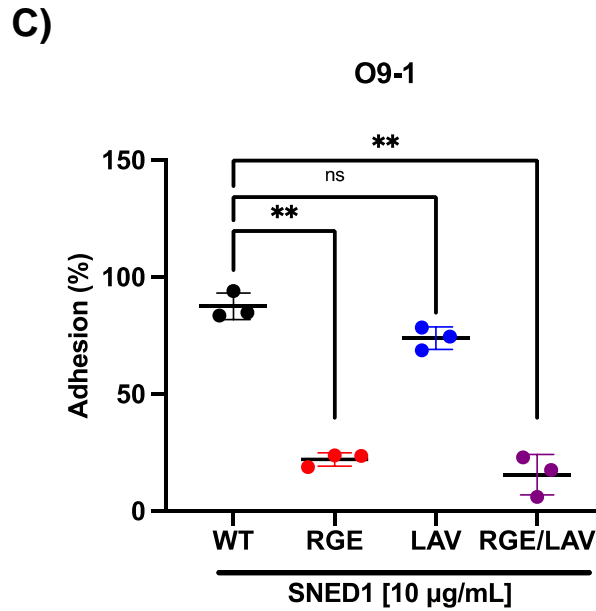
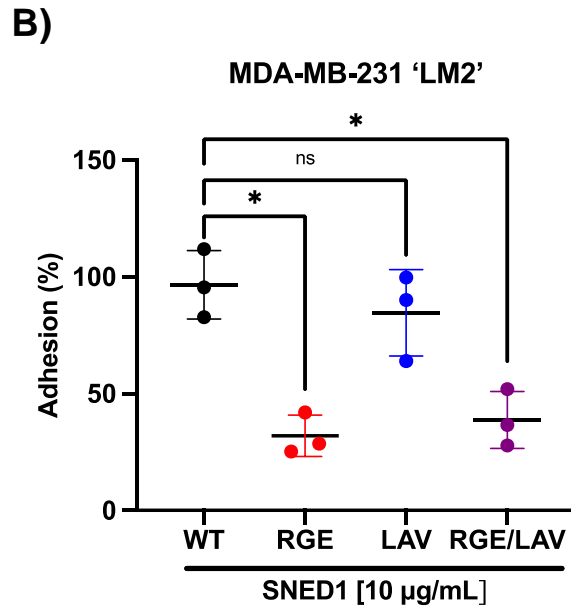
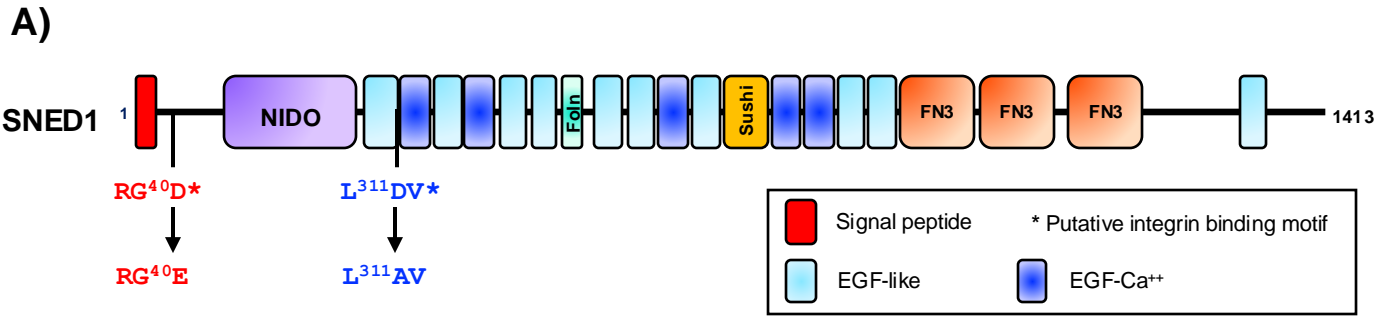


Figure 4: Functional blocking of integrins decreases cell adhesion to SNED1

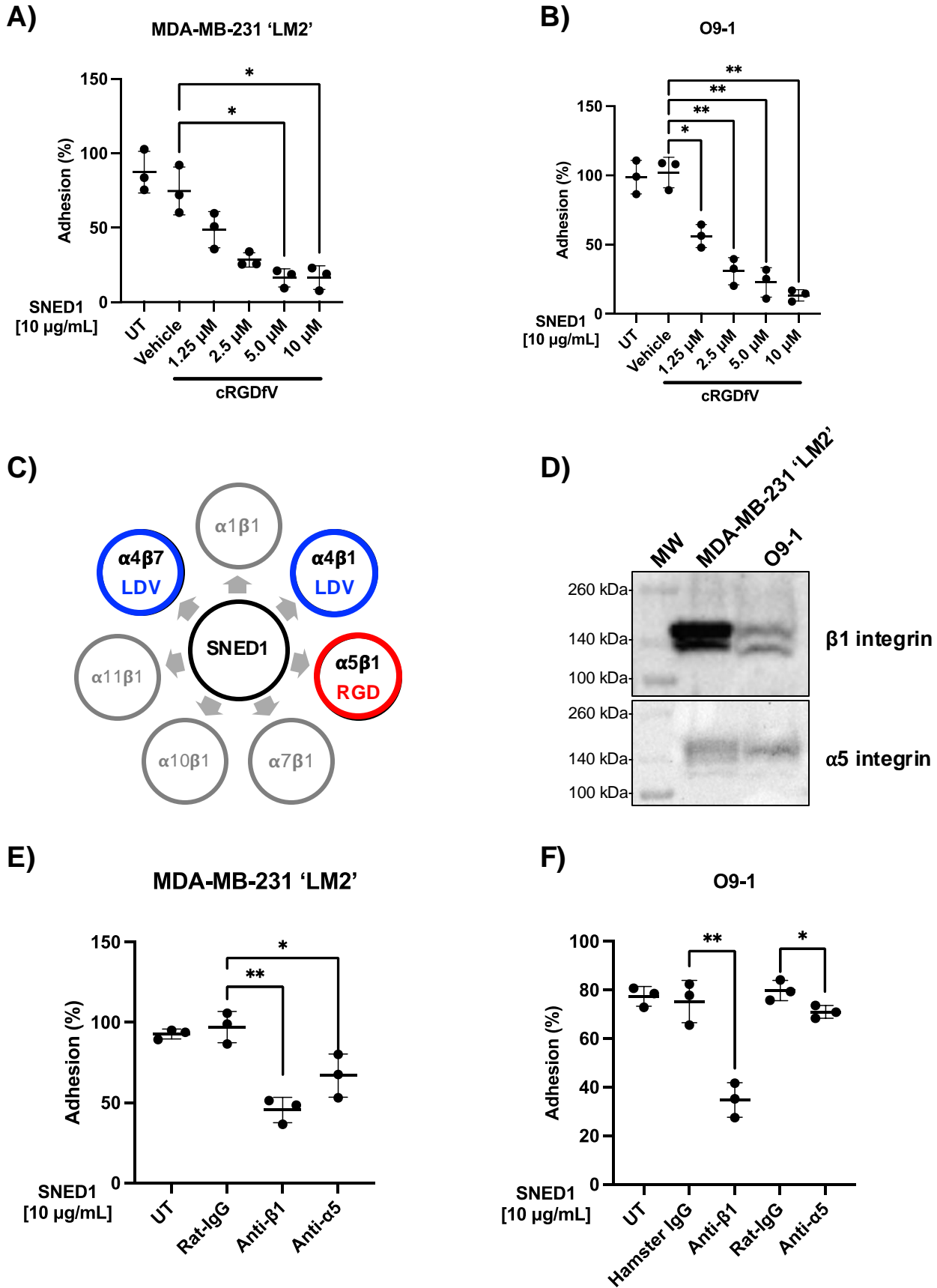


Figure S1. Cell adhesion on human SNED1 and murine Sned1

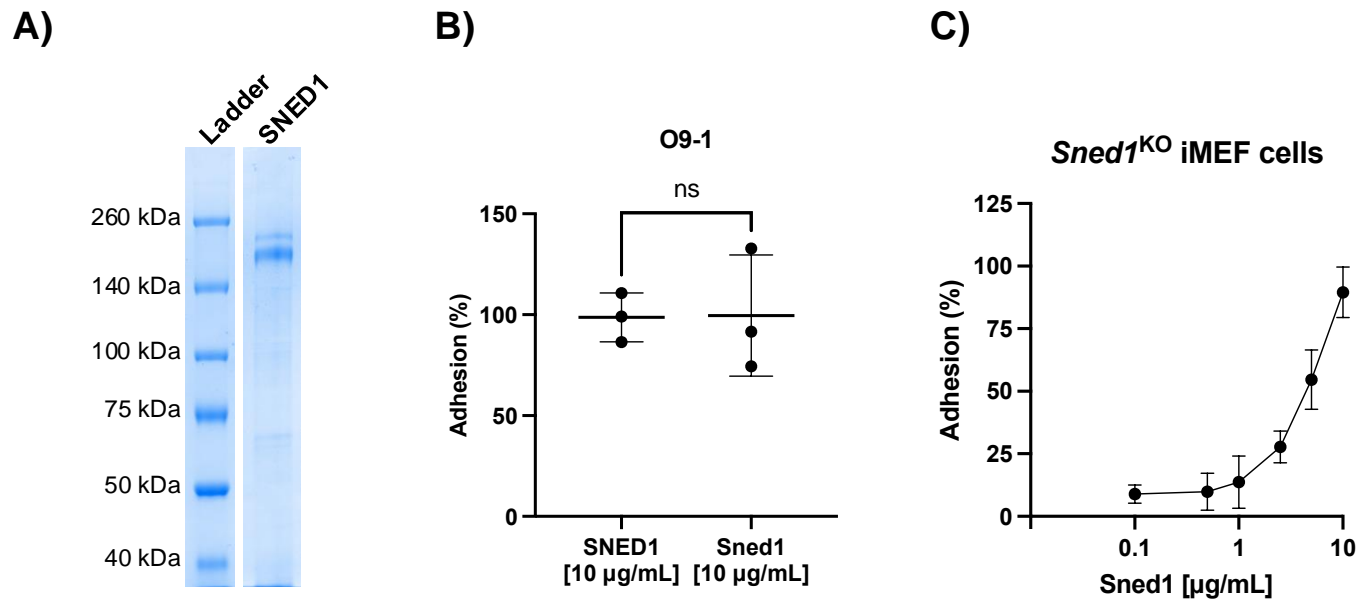


Figure S2. Purification of integrin binding mutants of SNED1

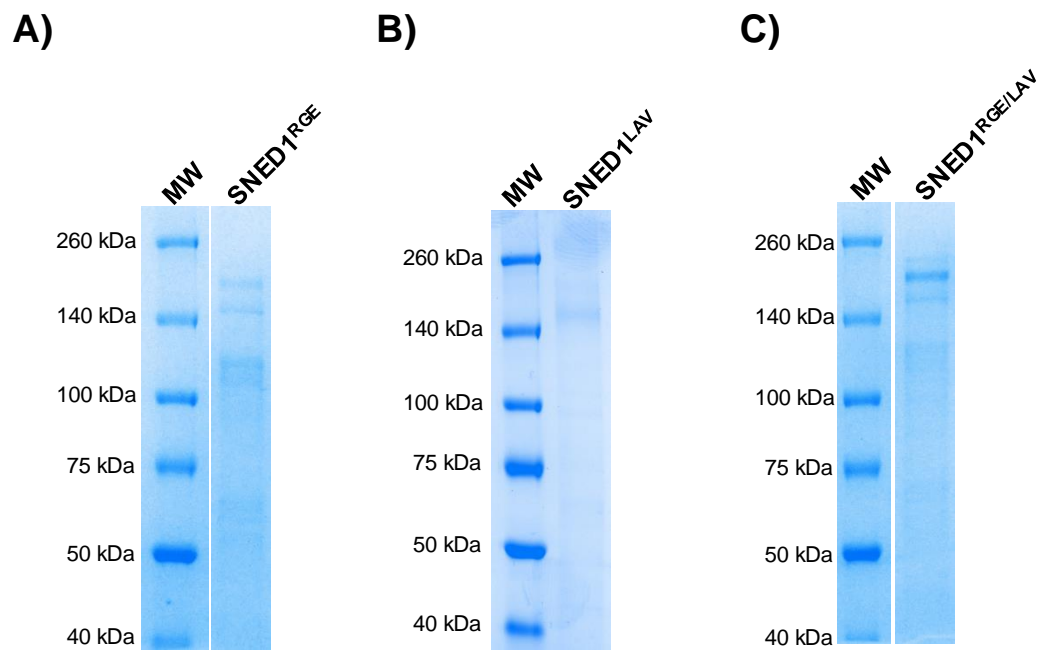


Figure S3. The RGD motif in SNED1¹⁻²⁶⁰ is required for cell adhesion

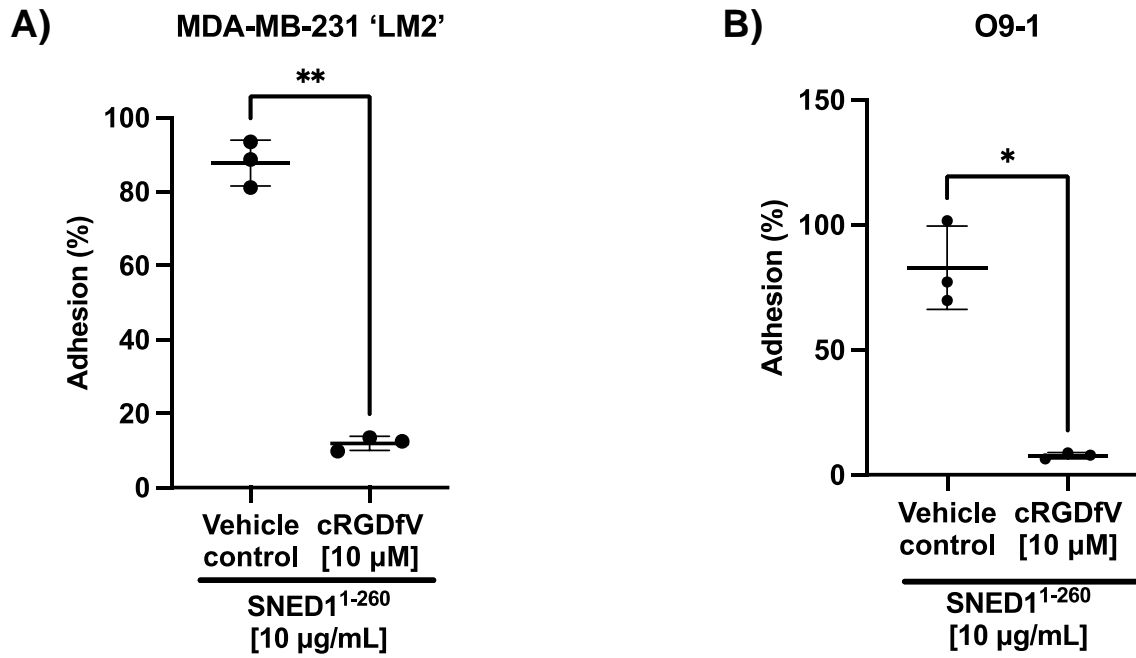
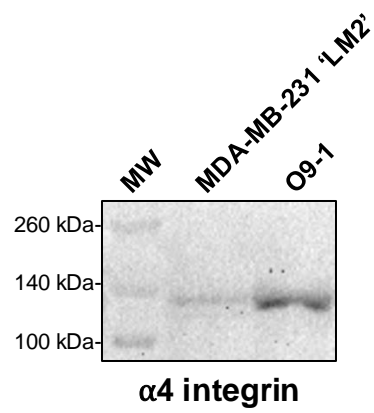
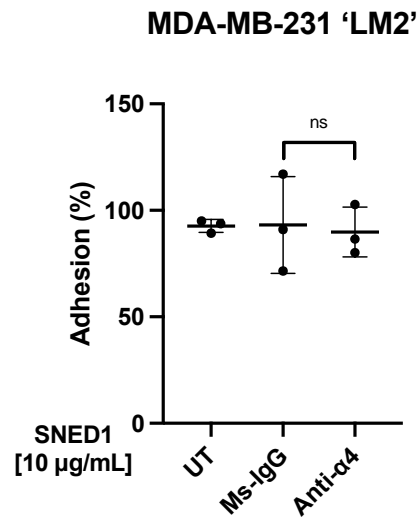


Figure S4. Functional blocking of $\alpha 4$ integrin does affect breast cancer cell adhesion to SNED1

A)



B)



Supplementary Table 1: List of primers

Primer	Sequence	Purpose
BglII-KOZAK-ATG-SNED1Hs_F	5' TCGAAGATCTGCCACCATGCGGCACGGCGTCGC 3'	Subcloning SNED1 into retroviral pMSCV-IRES-Hygro vector
HpaI-Stop-His-SNED1Hs_R	5'GATGTTAACCTAGTGGTGATGGTGATGATGAGATTTCTCCAGTGTCTGACTCT TACT 3'	Shuttling of SNED1-His WT, RGE, LAV, or GE/LAV) into retroviral pMSCV-IRES-Hygro vector
HpaI-Stop-FLAG-NFS_R	5' CCGTAACTTACTTGTCTCATCGTCTTTGTAGTCGCACTGGGGAGGCTCAC 3'	Subcloning SNED1 ¹⁻⁵⁷¹ into retroviral pMSCV-IRES-Hygro vector with the addition of a C-terminal FLAG tag
HpaI-Stop-FLAG-NF_R	5' CCGTAACTTACTTGTCTCATCGTCTTTGTAGTCGACGCAGAGGTAGCTCCC 3'	Subcloning SNED1 ¹⁻⁵³⁰ into retroviral pMSCV-IRES-Hygro vector with the addition of a C-terminal FLAG tag
SNED1_c120a_F	5' CCGAGCGCGGCGAAGCCGTCACC 3'	Introduction of the c120>a (pG40E) point mutation to generate SNED1 ^{RGE}
SNED1_c120a_R	5' GGTGACGGCTTCGCCGCGCTCGG 3'	
SNED1_a932c_F	5' GGAGGTGCCACCTGGCCGTGAACGAATGTGC 3'	Introduction of the a932>c (pD311A) point mutation to generate SNED1 ^{LAV}
SNED1_a932c_R	5' GCACATTCGTTACGGCCAGGTGGCACCTCC 3'	

Supplementary Table 2: List of antibodies used for functional blocking and immunoblotting

Antibody	Host species	Reactivity	Application	Concentration used ($\mu\text{g/mL}$)	Catalog #
Anti- β 1 Integrin	Rat	Human	Functional blocking	10	Sigma, MABT821
Anti- α 5 Integrin	Rat	Human	Functional blocking	10	Sigma, MABT820
Anti- α 4 Integrin	Mouse	Human	Functional blocking	10	Sigma, MAB1383
Anti- β 1 Integrin	Hamster	Mouse	Functional blocking	10	BD Biosciences, BDB555002
Anti- α 5 Integrin	Rat	Mouse	Functional blocking	10	Biologend, 103817
Rat IgG	Rat	Isotype control	Functional blocking	10	Invitrogen, PI31903
Mouse IgG	Mouse	Isotype control	Functional blocking	10	Invitrogen, PI31933
Hamster IgM	Hamster	Isotype control	Functional blocking	10	Biologend, 401014
Anti-SNED1	Rabbit	Human	Immunoblotting	1	Naba lab
Anti-His	Mouse	-	Immunoblotting	1	Sigma, SAB2702218
Anti-FLAG	Rabbit	-	Immunoblotting	1	Sigma, F7425
Anti- β 1 Integrin sera	Rabbit	Human, Mouse	Immunoblotting	1:1000 dilution	In-house
Anti- α 5 Integrin	Rabbit	Human, Mouse	Immunoblotting	0.217	Abcam, AB150361
Anti- α 4 Integrin	Rabbit	Human, Mouse	Immunoblotting	0.5	Invitrogen, MA5-27947